Pressure dependence of the resistivity around valence transition based on $1/N$-expansion study for extended Anderson lattice

Yasutaka NISHIDA [*] and Tomokazu OOKUBO [†]

Department of Materials Engineering Science,
Graduate School of Engineering Science, Osaka University,
Toyonaka, Osaka 560-8531

We investigate the behavior of the resistivity around valence transition in the one-dimensional extended periodic Anderson model (PAM) with the Coulomb repulsion between f and conduction electron U_{fc}. By using $1/N$-expansion in the leading order in $(1/N)^0$, where N is the spin-orbital degeneracy of f-electrons, valence transition happens at critical U_{fc} with increasing the atomic f-level as seen in the previous work.[5] We calculate the resistivity whole temperature range around valence transition based on the extended PAM including the crystal field and investigate how the physical properties such as Kondo temperature is modified by additional U_{fc} interaction. As a result, the double peak structure of the electrical resistivity fades away rapidly by the rapid increase of the Kondo temperature.

1. Introduction

Heavy Fermion Systems have been investigated extensively both experimentally and theoretically as typical system of strongly correlated electrons. In 1979 Steglich and collaborators discovered an intermetallic of the rare earth metal cerium $CeCu_2Si_2$,[1] which is well known as first discovered superconductor with $T_c \sim 0.7$K at ambient pressure. In the phase diagram in P-T plane of $CeCu_2Si_2$ under the high pressure, two superconducting transition temperature is confirmed. The isostructual compound, $CeCu_2Ge_2$,[2,3] also has the same phase diagram.

These two compounds have been considered to have the similar physical properties if the origin of the pressure for $CeCu_2Si_2$ is shifted. According to the recent experimental research,[4] the mechanism of the the superconductivity at higher pressure region is seemed to be different from the ordinary antiferromagnetic spin fluctuation, because transition temperature is away from the point of magnetic instability at $T = 0$. Around the superconducting transition temperature at higher pressure P_c, the residual resistivity has a peak, and the coefficient of T^2-term of the resistivity shows rapid decrease. At high temperature, two temperatures corresponding to maxima of the magnetic resistivity coincides around P_c. From these results, these coincidence around P_c seemed to be related to a rapid change of valence of Ce,[5,6] so that the superconductivity mediated by the valence fluctuation was proposed.

In this short paper, we study the pressure dependence of the resistivity based on the pioneering work[5] on the valence fluctuation by the extended periodic Anderson model with f-c coulomb repulsion U_{fc}. Then, we use $1/N$-expansion[7–9] for extended Anderson lattice including crystal field, calculate both the low temperature region

($T \leq T_K/10$, where T_K is the Kondo temperature.) and the high temperature region ($T \geq T_K$) within $(1/N)^0$. In the case of $U_{fc} = 0$, the double peak structure due to the crystal field is shown to merge into single peak gradually with increasing $\varepsilon_f (< 0)$. On the other hand, in the case of $U_{fc} \neq 0$, we find that the double peak structure fades away more rapidly due to the increase of T_K caused by rapid change of n_f.

The paper is organized as follows. In §2, we introduce the model Hamiltonian and $1/N$-expansion. In § 3 and 4, we show the result the physical properties both low and high temperature region, and the pressure dependence of the resistivity. In section 5, we summarize conclusions and remarks.

2. Model and Formal Preliminaries

In this paper, we start with an extended periodic Anderson model, which is a periodic Anderson model (PAM) with f-electron in a manifold of $J = 5/2$,[10] and Coulomb repulsion between f and conduction electrons, U_{fc}: Our model Hamiltonian is given by

$$H = H_c + H_f + H_{hy} + H_{fc}, \tag{2.1}$$

$$H_c = \sum_{\mathbf{k}\sigma} \varepsilon_{\mathbf{k}\sigma} c^{\dagger}_{\mathbf{k}\sigma} c_{\mathbf{k}\sigma}, \tag{2.2}$$

$$H_f = \sum_{i\Gamma} E_{i\Gamma} f^{\dagger}_{i\Gamma} f_{i\Gamma}, \tag{2.3}$$

$$H_{hy} = \frac{1}{\sqrt{N_L}} \sum_{\sigma,i,\mathbf{k},\Gamma} (V_{\mathbf{k}\Gamma\sigma} e^{-i\mathbf{k}\cdot\mathbf{R}_i} c^{\dagger}_{\mathbf{k}\sigma} f_{i\Gamma} b^{\dagger}_i + \text{h.c.}), \tag{2.4}$$

$$H_{fc} = U_{fc} \sum_{i,\Gamma} n^{f}_{i\Gamma} n^{c}_i, \tag{2.5}$$

where, $c^{\dagger}_{\mathbf{k}\sigma}$ is the creation operator for the conduction electron with wave vector $\mathbf{k}$ and spin σ, and $\varepsilon_{\mathbf{k}\sigma}$ is the energy of the conduction electron with wave vector $\mathbf{k}$ and spin σ. N_L denotes the number of the lat-

---
[*] E-mail address: y-nishida@blade.mp.es.osaka-u.ac.jp
[†] E-mail address: ookubo@blade.mp.es.osaka-u.ac.jp

tice site, and i stands for the site index. Furthermore we introduce the slave-boson which represents the f^0-state, and pseudo-fermion which represents f^1-state, following the Coleman: $b_i^\dagger$ is the creation operator for the slave-boson at i-site, $f_{i\Gamma}^\dagger$ is the creation operator for the pseudo-fermion at i-site with Crystalline-Electric-Field (CEF) level $|\Gamma\rangle$. The mixing potential $V_{\mathbf{k}\Gamma\sigma}$ is expressed as $V_{\mathbf{k}\Gamma\sigma} = \sum_M O_{\Gamma M} V_{\mathbf{k}M\sigma}$, M is the z-component of angular momentum J of an f-electron: $M = J_z(J = 5/2)$. Using the spherical harmonic function Y_l^m, $V_{\mathbf{k}M\sigma}$ is given by

$$V_{\mathbf{k}M\sigma} = V_0\sqrt{\frac{4\pi}{3}}\left\{-2\sigma\sqrt{\frac{(\frac{7}{2}-2M\sigma)}{7}}Y_{l=3}^{M-\sigma}(\theta_k, \phi_k)\right\}. \tag{2.6}$$

$O_{\Gamma M}$ is determined by the symmetry of the crystal field. In tetragonal symmetry we can put each f-level as follows,

$$E_{i|\pm1\rangle} = \varepsilon_f + \Delta_2, \; E_{i|\pm2\rangle} = \varepsilon_f + \Delta_1, \; E_{i|\pm3\rangle} = \varepsilon_f. \tag{2.7}$$

where, the CEF splitting is parameterized by $\Delta_{1,2}$.

Here the on-site Coulomb repulsion U between f-electrons is assumed to be infinite, so that we must impose the following local constraints in order to guarantee an equivalence between the present model Hamiltonian,

$$\hat{Q}_i = b_i^\dagger b_i + \sum_\Gamma f_{i\Gamma}^\dagger f_{i\Gamma} = 1. \tag{2.8}$$

The expectation value of an operator $\hat{O}$ under the local constraint eq. (2.8) is given as[11]

$$\langle\hat{O}\rangle = \lim_{\{\lambda_i\}\to\infty}\langle\hat{O}\prod_i\hat{Q}_i\rangle_\lambda/\langle\prod_i\hat{Q}_i\rangle_\lambda, \tag{2.9}$$

where $\langle\hat{A}\rangle_\lambda$ is calculated in the grand canonical ensemble for the Hamiltonian H_λ:

$$\langle\hat{A}\rangle_\lambda \equiv \mathrm{Tr}\left[e^{-\beta H_\lambda}\hat{A}\right]/\mathrm{Tr}\left[e^{-\beta H_\lambda}\right], \tag{2.10}$$

$$H_\lambda = H + \sum_i\lambda_i\hat{Q}_i. \tag{2.11}$$

The single-particle Green function $G_{\mathbf{k}\sigma}$ for the conduction electron, B_i for the slave boson and $F_{i\Gamma}$ for the pseudo-fermion is given as follows:

$$G_{\mathbf{k}\sigma}(i\omega_n) = (i\omega_n - \varepsilon_{\mathbf{k}\sigma} - \Sigma_{\mathbf{k}\sigma}(i\omega_n))^{-1}, \tag{2.12}$$

$$B_i(i\nu_n) = (i\nu_n - \lambda_i - \Pi_i(i\nu_n))^{-1}, \tag{2.13}$$

$$F_{i\Gamma}(i\omega_n) = (i\omega_n - E_{i\Gamma} - \lambda_i)^{-1}. \tag{2.14}$$

The self-energies $\Sigma_{\mathbf{k}\sigma}$ and Π_i is calculated by $1/N$-expansion procedure. We perform an extended calculation on the basis of the modified version of $1/N$-expansion method.[9] In the lowest order, the Dyson equations for one-particle Green's function are given by the diagram shown in Fig. 1. Then the analytic form of the self-energy is given by

$$\Sigma_{\mathbf{k}\sigma}(i\omega_n) = \lim_{\lambda_i\to\infty}\left[-\sum_\Gamma|V_{\mathbf{k}\Gamma\sigma}|^2T\sum_{\nu_n}B_i(i\nu_n)\right.$$
$$\left.\times F_{i\Gamma}^0(i\omega_n + i\nu_n)/\langle\hat{Q}_i\rangle_\lambda\right], \tag{2.15}$$
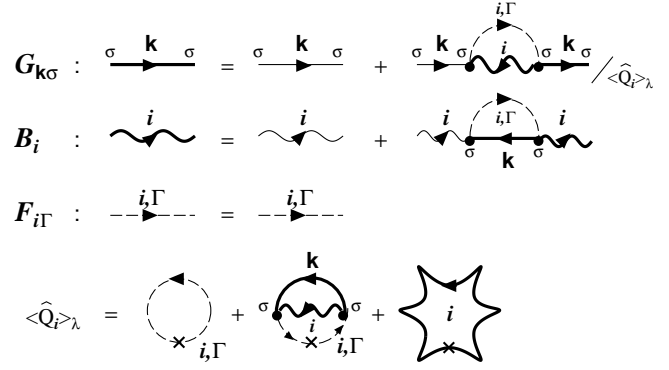

Fig. 1.   Diagrammatic representation of Dyson equations for single Green function within accuracy of $(1/N)^0$. Solid line denotes the conduction electron propagator, wavy line the slave-boson propagator and dashed line the pseudo-electron propagator, respectively.

$$\Pi_i(i\nu_n) = \frac{1}{N_L}\sum_\Gamma\sum_\sigma\sum_{\mathbf{k}_\sigma}|V_{\mathbf{k}\Gamma\sigma}|^2T\sum_{\omega_n}G_{\mathbf{k}\sigma}(i\omega_n)$$
$$\times F_{i\Gamma}^0(i\omega_n + i\nu_n), \tag{2.16}$$

$$\langle\hat{Q}_i\rangle_\lambda = \sum_\Gamma\langle\hat{n}_{fi\Gamma}\rangle_\lambda + \langle\hat{n}_{bi}\rangle_\lambda. \tag{2.17}$$

where

$$\langle\hat{n}_{fi\Gamma}\rangle_\lambda = \langle f_{i\Gamma}^\dagger f_{i\Gamma}\rangle_\lambda, \tag{2.18}$$

and

$$\langle\hat{n}_{bi}\rangle_\lambda = \langle b_i^\dagger b_i\rangle_\lambda. \tag{2.19}$$

By solving the coupled self-consistent equations eqs. (2.12)-(2.14) over the whole temperature range, we can discuss the temperature dependence of the physical quantities. In the next section, we discuss the physical properties at $T = 0$ as first step.

3. Physical properties at low temperature limit

At lower temperatures than the coherence temperature T_0, the coupled self-consistent equations become more simplified, with the help of the following relation,

$$-\frac{1}{\pi}\mathrm{Im}B_i(\omega + i0_+) \simeq a\delta(\omega - \lambda_i - \varepsilon_f + E_0) + C(\omega), \tag{3.1}$$

where, E_0 and a are the binding energy and residue of the slave-boson, respectively, and $C(\omega)$ is continuum part, which is non-zero $\omega \geq \lambda_i + \varepsilon_f$. E_0 corresponds to the Kondo temperature T_K, and the coherence temperature T_0 is estimated with $E_0/10$. E_0 and a are determined by the relation as

$$E_0 = \varepsilon_f - \mathrm{Re}\Pi_i(\lambda_i + \varepsilon_f - E_0) \tag{3.2}$$

$$\frac{1}{a} = 1 - \frac{d}{d\omega}(\mathrm{Re}\Pi_i(\omega))\Big|_{\omega=\lambda_i+\varepsilon_f-E_0} \tag{3.3}$$

Here we treat U_{fc} term with the Hartree-Fock approximation in $O((1/N)^0)$.[12] By using eq. (3.1), the system is in the coherent regime with the renormalized bands

given by

$$G_{\mathbf{k}\sigma}(i\omega_n) = \sum_{j=1}^{4} \frac{\tilde{A}_{\mathbf{k}\sigma}^{j}}{i\omega_n - \tilde{\alpha}_{\mathbf{k}\sigma}^{j}} \qquad (3.4)$$

with

$$\tilde{\varepsilon}_{\mathbf{k}\sigma} = \varepsilon_{\mathbf{k}\sigma} + U_{\mathrm{fc}}n_f, \qquad (3.5)$$

$$\tilde{\alpha}_{\mathbf{k}\sigma}^{j} = \tilde{\varepsilon}_{\mathbf{k}\sigma} + \mathrm{Re}\Sigma_{\mathbf{k}\sigma}(\tilde{\alpha}_{\mathbf{k}\sigma}^{j}), \qquad (3.6)$$

$$\tilde{A}_{\mathbf{k}\sigma}^{j} = \frac{(\tilde{\alpha}_{\mathbf{k}\sigma}^{j} - E_0)(\tilde{\alpha}_{\mathbf{k}\sigma}^{j} - E_0 - \Delta_1)(\tilde{\alpha}_{\mathbf{k}\sigma}^{j} - E_0 - \Delta_2)}{(\tilde{\alpha}_{\mathbf{k}\sigma}^{j} - \tilde{\alpha}_{\mathbf{k}\sigma}^{j+1})(\tilde{\alpha}_{\mathbf{k}\sigma}^{j} - \tilde{\alpha}_{\mathbf{k}\sigma}^{j+2})(\tilde{\alpha}_{\mathbf{k}\sigma}^{j} - \tilde{\alpha}_{\mathbf{k}\sigma}^{j+3})}, \qquad (3.7)$$

where, $\tilde{\alpha}_{\mathbf{k}\sigma}^{j} = \tilde{\alpha}_{\mathbf{k}\sigma}^{j+4}$.

Hence the self-consistent equations eqs. (2.12)-(2.14) are written by

$$E_0 - \varepsilon_f = \frac{1}{N_L} \sum_{j=1}^{4} \sum_{\Gamma} \sum_{\sigma} \sum_{\mathbf{k}_\sigma} \frac{\tilde{A}_{\mathbf{k}\sigma}^{j}|V_{\mathbf{k}\Gamma\sigma}|^2 f(\tilde{\alpha}_{\mathbf{k}\sigma}^{j})}{E_0 + \tilde{E}_{i\Gamma} - \varepsilon_f - \tilde{\alpha}_{\mathbf{k}\sigma}^{j}}, \qquad (3.8)$$

$$\frac{1}{a} = 1 + \frac{1}{N_L} \sum_{j=1}^{4} \sum_{\Gamma} \sum_{\sigma} \sum_{\mathbf{k}_\sigma} \frac{\tilde{A}_{\mathbf{k}\sigma}^{j}|V_{\mathbf{k}\Gamma\sigma}|^2 f(\tilde{\alpha}_{\mathbf{k}\sigma}^{j})}{(E_0 + \tilde{E}_{i\Gamma} - \varepsilon_f - \tilde{\alpha}_{\mathbf{k}\sigma}^{j})^2}, \qquad (3.9)$$

$$n = n_c + n_f = \frac{1}{N_L} \sum_{j=1}^{4} \sum_{\sigma} \sum_{\mathbf{k}_\sigma} f(\tilde{\alpha}_{\mathbf{k}\sigma}^{j})\tilde{A}_{\mathbf{k}\sigma}^{j} + (1-a). \qquad (3.10)$$

and

$$\tilde{E}_{i\Gamma} = E_{i\Gamma} + U_{\mathrm{fc}}n_c, \qquad (3.11)$$

where n, n_c, and n_f is the total electron number, the number of the conduction electrons, and f-electrons per site, respectively. Finally, the binding energy E_0, the residue a and other physical properties at $T = 0$ are obtained from a series of equations eqs. (3.8)-(3.10).

3.1 f-electron number

In this section, we show the f-electron number n_f per site as a function of the atomic f-level ε_f for series of CEF splitting scheme with U_{fc}. At first, let us investigate the trivial case, $V^2 \equiv \sum_\sigma |V_{\mathbf{k}\Gamma\sigma}|^2 = 0.98 \times 10^{-2}D^2$, $n = n_c + n_f = 1.4$, and $\Delta_1 = \Delta_2 = 0.6D$. Then the grand state is doublet ($N_{\mathrm{GS}} = 2$) state, so that, in Fig. 2, we find that if $\varepsilon_f \lesssim -0.6$, $n_f \sim 1$. However in case of $V^2 = 2.8 \times 10^{-2}$, n_f decreases monotonously by increasing the width of the density of state of localized f-electrons due to hybridization effect. On the other hand, in the case of $\Delta_1 = \Delta_2 = 0$ ($N_{\mathrm{GS}} = 6$), n_f decreases monotonously. If N_{GS} is small, n_f shows a little sudden decrease with increasing ε_f.

Next, we show the $U_{\mathrm{fc}} \neq 0$ result in Fig. 3 and 4. In Fig. 3, we set $\Delta_1 = \Delta_2 = 0$ for simplicity. Then, n_f shows the rapid decrease gradually with increasing U_{fc}. This behavior was already obtained by the past pioneering work.[5] In Fig. 4, we set $\Delta_1 = 0, \Delta_2 = 0.3D$ and $\Delta_1 = \Delta_2 = 0.6D$ in order to consider the CEF effect. From these result we find n_f vs ε_f is not much modified qualitatively by CEF effect.
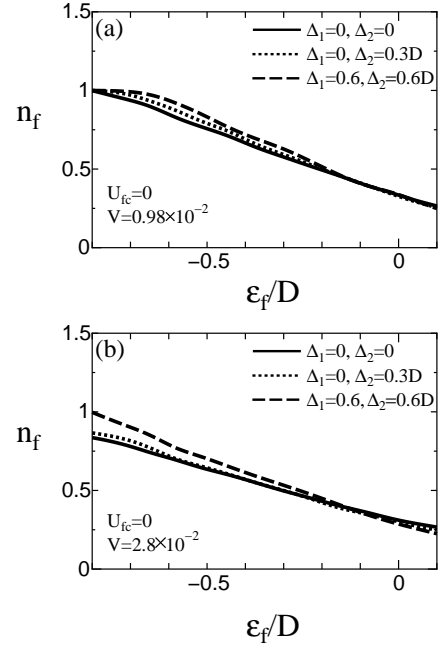

Fig. 2. (a) n_f vs ε_f in the case of $n = 1.4$, $U_{\mathrm{fc}} = 0$ and $V^2 = 0.98 \times 10^{-2}D^2$ for a series of CEF splittings. (b) n_f vs ε_f in the case of $n = 1.4$, $U_{\mathrm{fc}} = 0$ and $V^2 = 2.8 \times 10^{-2}D^2$ for a series of CEF splittings.
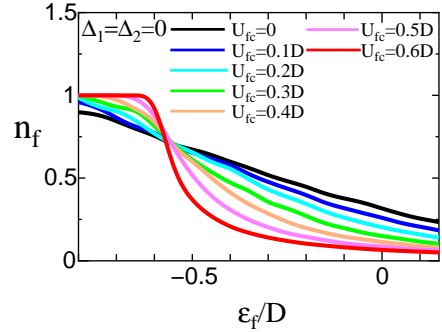

Fig. 3. n_f vs ε_f in the case of $n = 1.4$, $V^2 = 2.0 \times 10^{-2}D^2$ and $\Delta_1 = \Delta_2 = 0$ for a series of U_{fc}.

3.2 Kondo temperature

The Kondo temperature corresponds to the binding energy of the slave-boson E_0 in lattice case. We present the solution E_0 for the series of the self-consistent equations (3.8)-(3.10) within the $O((1/N)^0)$. Incidentally E_0 can be written as follows in the case of impurity without CEF effect and U_{fc},

$$E_0 = D\exp\left(\frac{\varepsilon_f}{6\rho_0 V^2}\right), \qquad (3.12)$$

where we impose the condition that $D \gg |\varepsilon_f| \gg E_0$. In eq. (3.12), 6 means the degeneracy of f-electron in a manifold $J = 5/2$, and ρ_0 represents for the density of state of the conduction electron per spin.

In Fig. 5, we show the result of E_0 vs ε_f for the various U_{fc} and CEF splitting. At first we again consider the trivial case $\Delta_1 = \Delta_2 = 0$ and $U_{\mathrm{fc}} = 0$. Then, E_0 increase gradually with increasing $\varepsilon_f(< 0)$. This tendency is ex-
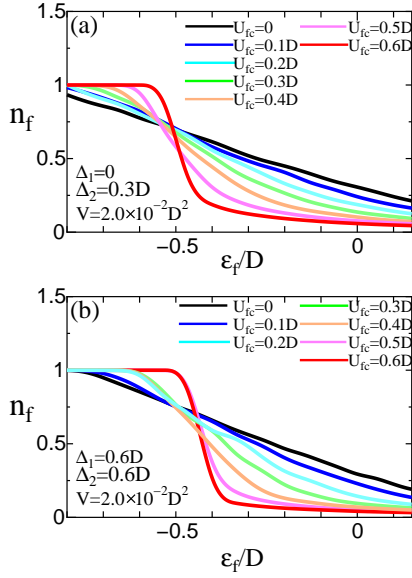
Fig. 4. (a) n_f vs ε_f in the case of $n = 1.4$, $V^2 = 2.0 \times 10^{-2}D^2$, $\Delta_1 = 0$, and $\Delta_2 = 0.3D$ for a series of U_{fc}. (b) n_f vs ε_f in the case of $n = 1.4$, $V^2 = 2.0 \times 10^{-2}D^2$, $\Delta_1 = 0.6D$, and $\Delta_2 = 0.6D$ for a series of U_{fc}.

pected from the impurity result eq. (3.12). Next, in case of $U_{\mathrm{fc}} \neq 0$, E_0 changes drastically as large as n_f with increasing ε_f. This is explained by the enhancement of the renormalization factor q accompanying with the rapid valence change. The renormalization factor q derived from mean-field[13] and Variational Monte Calro[14] is obtained as follows

$$q^{-1} = \frac{1 - n_f/2}{1 - n_f}. \tag{3.13}$$

The rapid change $n_f : 1 \rightarrow 0$ causes also the rapid enhancement of q, so that the Kondo temperature is enhanced around valence transition.
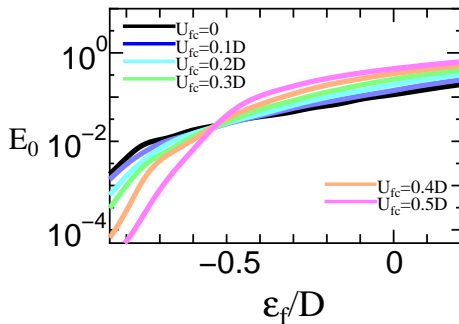

Fig. 5. E_0 vs ε_f in the case of $n = 1.4$, $V^2 = 2.0 \times 10^{-2}D^2$, $\Delta_1 = \Delta_2 = 0$ for a series of U_{fc}.

In Fig. 6, we illustrate the result of the $\Delta_1 = \Delta_2 = 0.0$ and $\Delta_1 = \Delta_2 = 0.6D$ under the condition $U_{\mathrm{fc}} = 0$. In the previous subsection, we find the CEF effect does not affect the ε_f dependence of n_f, on the other hand, Kondo temperature E_0 is greatly influenced of CEF effect. The value of the Kondo temperature depends much by the
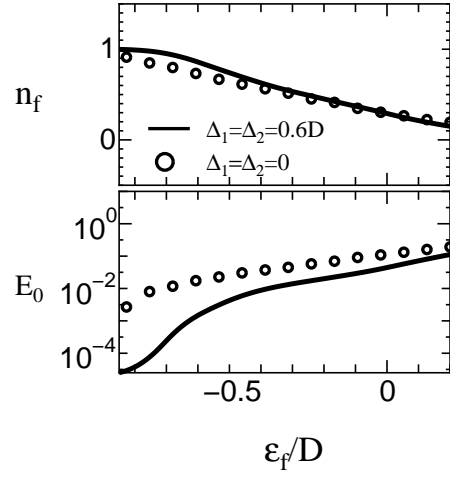
degeneracy of the localized f-electrons.

Fig. 6. n_f vs ε_f and E_0 vs ε_f in the case of $n = 1.4$, $V^2 = 2.0 \times 10^{-2}D^2$. The result of $\Delta_1 = \Delta_2 = 0.6D$ is shown by solid line, and that of $\Delta_1 = \Delta_2 = 0$ is shown by enclosed circle.

4.   Electrical Resistivity

In this section, the effect of the pressure on the temperature dependence of the resistivity is discussed. The pressure effect is parameterized as the atomic f-level ε_f measured from the band center of conduction electrons. The conductivity is obtained by means of the Kubo formula. By omitting some constant factors, we define the reduced conductivity,

$$\sigma = \frac{1}{N_L} \sum_{\sigma, \mathbf{k}} v_{\mathbf{k}}^2 \int d\varepsilon \left(-\frac{\partial f(\varepsilon)}{\partial \varepsilon}\right) \left[\mathrm{Im}G_{\mathbf{k}\sigma}(\varepsilon + \mathrm{i}0_+)\right]^2,$$
$$\tag{4.1}$$

where we use the renormalized Green function derived from $1/N$-expansion procedure. In order to calculate the resistivity $1/\sigma$ over the whole temperature range, we must solve the Dyson equation eqs. (2-12)-(2.14) self-consistently (self-consistent $1/N$).

We illustrate the result of the calculation for the series of ε_f in Fig. 7 The parameters are adopted as $D=1$(band width), $V^2 \equiv \sum_\sigma |V_{\mathbf{k}\Gamma\sigma}|^2 = 1.28 \times 10^{-2}D^2$, $n = n_c + n_f = 1.4$, and set the CEF parameter as $\Delta_1 = 0.015D$ and $\Delta_2 = 0.038D$ putting the case of $CeCu_2Si_2$.[15]

In both case of $U_{\mathrm{fc}} = 0$ and $U_{\mathrm{fc}} \neq 0$, the double peak structure fades away with increasing $\varepsilon_f (< 0)$. The double peak structure of the temperature dependence is commonly shown to merge into a single peak with increasing pressure. These behaviors are consistent with the tendency observed in Ce-based heavy fermions. However, at the large ε_f (high pressure region), the position of the single peak of $1/\sigma$ differs much in both cases. In case of $U_{\mathrm{fc}} = 0$, the peak position does not change much at large ε_f. On the other hand, in case of $U_{\mathrm{fc}} \neq 0$, the peak position changes much with increasing ε_f. The Fig. 9 shows this situation clearly, i.e., rapid increase of E_0 (Kondo temperature) happens around the valence transition. Under the condition without U_{fc}, the Kondo tem-
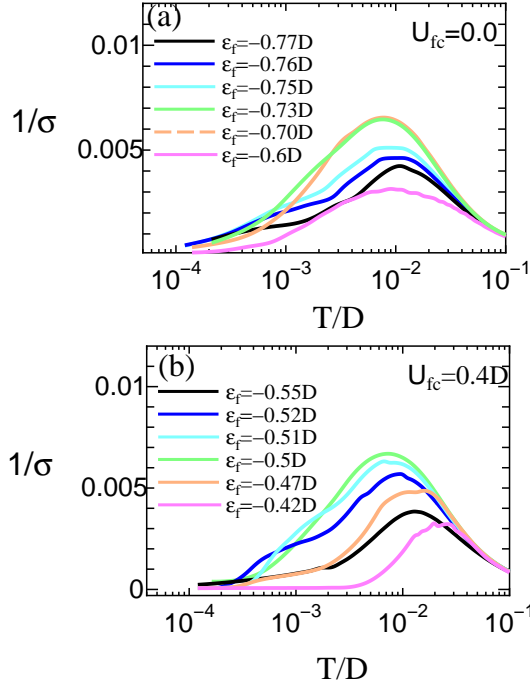
Fig. 7. (a) The temperature dependence of electrical resistivity for a series of the atomic f-level in the case of $U_{fc} = 0$ and (b) that in the case of $U_{fc} = 0.4D$. The CEF splittings are set as $\Delta_1 = 0.015D$ and $\Delta_2 = 0.038D$ in both cases.
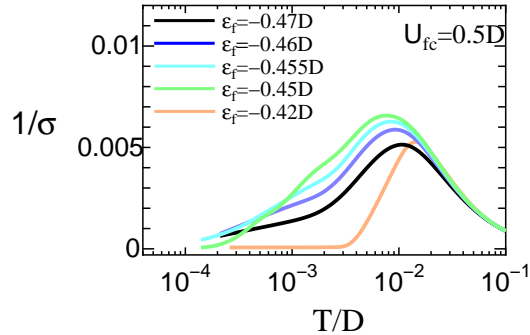

Fig. 8. The temperature dependence of electrical resistivity for a series of the atomic f-level in the case of $U_{fc} = 0.5D$.

perature increases slowly with increasing ε_f compared with the case of $U_{fc} = 0.4D$. The effect of the additional term U_{fc} seems to promote the merging of the double peak structure of the resistivity.

We also illustrate the result in case of $U_{fc} = 0.5D$ in Fig. 8. We find that the electrical resistivity becomes more sensitive to the change of ε_f than that of $U_{fc} = 0$.

5. Conclusion

We have studied the behavior of the pressure dependence of the electrical resistivity around valence transition based on $1/N$-expansion for extended periodic Anderson lattice including CEF effect. This is the extended calculation of the pioneering work.[5] At lower temperature than Kondo temperature, the result of n_f vs ε_f does not change qualitatively, i.e., n_f shows the rapid decrease with increasing U_{fc} where CEF effect does not
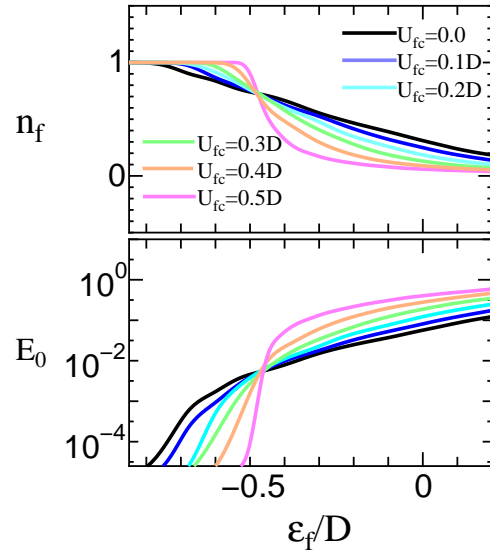

Fig. 9. n_f vs ε_f and E_0 vs ε_f in the case of $n = 1.4$, $V^2 = 1.28 \times 10^{-2} D^2$, $\Delta_1 = 0.015D$ and $\Delta_2 = 0.038D$ for the series of U_{fc}.

affect the tendency of the change of n_f as a function of ε_f. remarkably. However the Kondo temperature T_K shows different behavior by CEF effect, because T_K depends on the degeneracy of the localized f-electrons much. Moreover, we have calculated the electrical resistivity over the whole temperature region by solving the Dyson equation self-consistently within $(1/N)^0$ and investigated the effect of the additional interaction U_{fc} to the temperature dependence of the electrical resistivity.

As a result, we found that the double peak structure of the resistivity due to the crystal field fades away more rapidly caused by the rapid change of n_f. Especially, in the region of ε_f around the valence transition, the resistivity show the drastic change by a minute change of ε_f. The effect of the additional term U_{fc} promote the merging of the double peak structure of the resistivity. This tendency may be consistent with the merge of the resistivity right above P_c in the phase diagram in P-T plane of CeCu$_2$Si$_2$ or CeCu$_2$Ge$_2$.

Finally we point out some remaining problem and perspectives. In our calculation, the term of U_{fc} is treated within Hartree-Fock approximation, so that the effect of U_{fc} may be overestimated by the present calculation. In order to discuss the problem more qualitatively, we need more proper approximation. Experimentally, the rapid decrease of Kadowaki-Woods ratio is observed around P_c. This suggests that the system is changed from Kondo regime to the valence fluctuation regime rapidly. We can discuss this problem by studying up to $(1/N)^1$, where intersite correlation can be discussed. By investigating between the change of the degeneracy of the f-electron and pressure effect or U_{fc}, we may also discuss the mechanisms of enhancement of T_K in detail.

Acknowledgement

1) F. Steglich, J. Aarts, C. D. Bredl, W. Lieke, D. Meschede, W. Franz, and H. Schäfer: Phys. Rev. Lett. **43** (1979) 1892.
2) D. Jaccard, E. Vargoz, H. Wilhelm, and K. Alami-Yadri: Rev. High Pressure Sci. Technol. **7** (1998) 412.
3) D. Jaccard, H. Wilhelm, K. Alami-Yadri and E. Vargoz: Physica B **259-261** (1999) 1.
4) A. T. Holems, D. Jaccard and K. Miyake: Phys. Rev. B **69** (2004) 024508.
5) Y. Onishi and K. Miyake: J. Phys. Soc. Jpn. **69** (2000) 3955.
6) K. Miyake and H. Maebashi: J. Phys. Soc. Jpn. **71** (2002) 1007.
7) Y. Ōno, T. Matsuura and Y. Kuroda: Physica C **159** (1989) 878.
8) Y. Ōno, T. Matsuura and Y. Kuroda: J. Phys. Soc. Jpn. **60** (1991) 3475.
9) Y. Nishida, A. Tsuruta and K. Miyake: J. Phys. Soc. Jpn. **75** (2006) 064706.
10) H. Kontani and K. Yamada: J. Phys. Soc. Jpn. **65** (1996) 172.
11) P. Coleman: Phys. Rev. B **29** (1984) 3035.
12) Dai S. Hirashima, Y. Ōno, T. Matsuura and Y. Kuroda: J. Phys. Soc. Jpn. **61** (1992) 649.
13) T. M. Rice and K. Ueda: Phys. Rev. B **34** (1986) 6420.
14) H. Shiba: J. Phys. Soc. Jpn. **55** (1986) 2765.
15) S. Horn, E. Holland-Moritz, M. Loewenhaupt, F. Steglich, H. Scheuer, A. Benoit, and J. Flouquet: Phys. Rev. B **23** (1981) 3171.